Korean J. Chem. Eng., 33(9), 2547-2554 (2016)
DOI: 10.1007/s11814-016-0112-8

pISSN: 0256-1115
eISSN: 1975-7220

CeO_2-TiO_2 catalyst prepared by physical mixing for NH_3 selective catalytic reduction: Evidence about the migration of sulfates from TiO_2 to CeO_2 via simple calcination

Inhak Song, Seunghee Youn, Hwangho Lee, and Do Heui Kim†

School of Chemical and Biological Engineering, Institute of Chemical Processes,
Seoul National University, Seoul 08826, Korea
(*Received 27 January 2016 • accepted 22 April 2016*)

Abstract−A mechanical mixture of CeO_2 and TiO_2 powder with a small amount of sulfate was applied for the selective catalytic reduction (SCR) of NO with NH_3. After calcination at 500 °C, the mixed sample showed significantly enhanced activity and selectivity compared to the uncalcined one and, moreover, demonstrated even higher activity than the conventional V_2O_5/TiO_2 catalyst above 300 °C. Combined characterization results revealed that the main active sites were newly formed sulfate species on CeO_2, the number of which increased with calcination. Temperature-resolved DRIFT spectra provided convincing evidence about the migration of sulfate species from TiO_2 to CeO_2, as confirmed from the shift of ν(S=O) band as a result of the mechanical mixing and the subsequent calcination.

Keywords: Selective Catalytic Reduction, Sulfation, CeO_2, TiO_2, Sulfate Migration

INTRODUCTION

More stringent regulations on NO_x emission have been implemented due to its harmfulness to environment and human health [1]. Selective catalytic reduction (SCR) of NO_x with NH_3 is the main technology for the after-treatment of NO_x emission from mobile or stationary source. Especially, vanadium-based catalysts, such as V_2O_5-WO_3/TiO_2 or V_2O_5-MoO_3/TiO_2, were successfully commercialized in removing NO_x from stationary source and are still being extensively studied [2,3]. However, several problems such as toxic vanadium leaching and N_2O formation in the conventional V-based catalyst led many research groups to pay attention to environmentally friendly catalysts, substituting vanadium with other transition metal oxides.

Solid acid catalysts containing sulfate or phosphate on the surface have been widely known as highly active for various catalytic processes [4,5]. Recently, several groups reported that sulfated CeO_2 also has excellent catalytic activity in SCR of NO_x with NH_3 [6-8]. Especially, Ce-based catalysts are known to have remarkable resistance to sulfur poisoning in SCR reaction [9,10], which is attributed to the strong interaction between sulfur and CeO_2 preserving the other active site. Wu et al. indicated that Ce doping was effective in enhancing SO_2 resistance of Mn/TiO_2 catalysts [10]. Therefore, unlike other catalysts which could be deactivated by sulfur species, CeO_2 showed significantly higher activity after sulfation [6]. Yang et al. investigated the mechanism over sulfated CeO_2 catalysts in SCR reaction [7], while Zhang et al. found that the NO removal activity of CeO_2 was strongly affected by sulfation temperature [8]. Although sulfated CeO_2 has received attention as the potential SCR catalyst because of the excellent properties, it must be pointed out that it was prepared by using either wet impregnation with $(NH_4)_2SO_4$ solution [11] or passing through CeO_2 with SO_2 gas for a long time [6-8]. Hence, such complex step of loading sulfate on CeO_2 remains as a challenge for industrial application.

This work was inspired by the commercially available TiO_2 with a small amount of sulfate, which could be the source of ceria sulfation. We investigated the use of a mechanical mixture of commercially available CeO_2 and TiO_2, and its calcined sample for the SCR of NO with NH_3, and elucidated the evidence on the surface migration of sulfate species from TiO_2 to CeO_2 particles.

EXPERIMENTAL

1. Sample Preparation

Anatase TiO_2 (DT-51 Millenium Chemicals, with the S content of 1.25 atomic % and surface area of 83 m^2/g) and CeO_2 (Rhodia, surface area of 131 m^2/g) were used as TiO_2 and CeO_2 samples, respectively. The CeO_2 and TiO_2 samples were applied to experiments without further treatment. CeO_2 and TiO_2 were mechanically mixed in a porcelain mortar for 15 min, and the mass ratio of CeO_2 to TiO_2 was 3 : 20 (designated as CeTi-mix). After mechanical mixing, the mixture was calcined at 500 °C for 4 h under ambient air (designated as CeTi-mix-cal). For reference, conventional V_2O_5/TiO_2 catalyst was prepared with wet impregnation method. Ammonium metavanadate (99%, Sigma Aldrich) was dissolved in oxalic acid solution to produce the solution of vanadium precursor, and 5 wt% V was deposited on the TiO_2 (DT-51) support. After impregnation, catalyst was dried and then calcined at 500 °C for 4 h under ambient air.

2. Characterization

Powder XRD patterns were taken using Ultra X18 (Rigaku) with

†To whom correspondence should be addressed.
E-mail: dohkim@snu.ac.kr
‡This paper is dedicated to Professor Seong Ihl Woo on the occasion of his retirement from Korea Advanced Institute of Science and Technology.

a Cu Kα radiation. Hydrogen temperature-programmed reduction (H_2-TPR) profile was obtained in a BEL-CAT-Basic instrument (BEL Japan Inc.). About 0.05 g of prepared samples was loaded on quartz wool bed in a quartz U-shaped reactor while checking the thermal conductivity of flowing gas. Scanning electron microscopy (SEM) and energy dispersive X-ray spectroscopy (EDS) investigations were carried out with JSM-6360 (JEOL) with the accelerating voltage of 20 kV. All samples were coated with Pt metal with MSC-101 (JEOL). NH_3 gas in NH_3-TPD profile was monitored with FT-IR spectroscopy (Nicolet 6700, Thermo Scientific) with a 2 m gas analysis cell. While 0.07 g of sieved samples was used for pure CeO_2 or TiO_2 sample, 0.14 g of samples was used for CeTi-mix-cal sample. All samples were pretreated at 500 °C in 2% O_2 balance with N_2 with the total flow rate of 200 mL/min for 1 h. Afterward, the samples were cooled to 80 °C and saturated with NH_3 until the surface was saturated with adsorbed NH_3, followed by N_2 purging at 80 °C for 1 h. Then the samples were cooled again to below 30 °C and purged by N_2 for 1 h, and the samples were heated to 600 °C at 10 °C/min in N_2 flow (200 mL/min). Thermal desorption of SO_2 was monitored with FT-IR spectroscopy (Nicolet 6700, Thermo Scientific) with a 2 m gas analysis cell while 0.2 g of samples was heated to 850 °C at 10 °C/min in 5% O_2 balanced with N_2 with the total flow rate of 200 mL/min. *In situ* DRIFT spectra were obtained with FT-IR spectroscopy (Nicolet 6700, Thermo Scientific) equipped with high-temperature DRIFT cell fitted with ZnSe windows. The powder samples were rigidly packed in a circular cell to prevent the collapse of samples during heating. The IR spectra were recorded by accumulating 32 scans at a resolution of 4 cm^{-1}.

3. Catalytic Activity Test

The prepared samples were sieved to select the particle size ranging from 300 to 500 μm prior to the activity measurement. Activity tests were in a fixed bed quartz tubular reactor with 0.15 g of sieved catalysts. The reaction gas consisted of 500 ppm NO, 500 ppm NH_3, 2% O_2 and 3% H_2O (when used) balanced with N_2. The total flow rate was 200 mL min^{-1} and the gas hourly space velocity (GHSV) was 80,000 mL g^{-1} h^{-1}. The reaction temperature was raised from 150 °C to 500 °C with the step of 50 °C, and activity results were obtained after reaching the steady state condition. NO_x concentration was measured by using NO_x chemiluminescence analyzer (42i High level, Thermo Scientific), and the concentration of N_2O was recorded from FT-IR spectroscopy (Nicolet 6700, Thermo Scientific) with a 2 m gas analysis cell. NO_x conversion was calculated based on the following equation:

$$NO_x \text{ conversion } (\%) = \frac{[NO_x]_{in} - [NO_x]_{out}}{[NO_x]_{in}} \times 100$$

RESULTS AND DISCUSSION

1. NH_3-SCR Activity Results

Prepared samples were applied for standard SCR reaction and their activity results are shown in Fig. 1. NO removal activity of CeO_2 was poor over the whole temperature range, which was similar to previously reported results [6]. NO_x conversion over CeO_2 gradually increased to about 30% as reaction temperature increased to 400 °C, but rapidly decreased above 400 °C. Also, the amount of N_2O emitted was more than 30 ppm from 400 °C to 500 °C. Meanwhile, pure TiO_2 revealed a negligible NO removal activity in the temperature below 400 °C; however, NO_x conversion rapidly increased up to 80% at 500 °C. In contrast to CeO_2 or TiO_2 catalysts, the mechanical mixture of TiO_2 and CeO_2 (CeTi-mix) exhibited much higher NO_x conversion than the sum of each NO conversion of pure CeO_2 or TiO_2 at a reaction temperature from 350 °C to 500 °C with the formation of N_2O below 10 ppm, implying that merely mixing of these two samples with a mortar for 15 min induced a new sample with improved activity and selectivity. Furthermore, the calcination of the mechanical mixture at 500 °C further enhanced activity with a wide operating window from 300 °C to 500 °C. In comparison with conventional V_2O_5/TiO_2 catalyst (dashed-line), CeTi-mix-cal catalyst exhibited a wide operating window, especially in the high temperature region, though NO_x conversion at low temperature was quite inferior to the former catalyst. Also, it is remarkable that, unlike the V_2O_5/TiO_2 catalyst which emitted a large amount of N_2O above 350 °C, N_2O emission was greatly suppressed below 10 ppm over CeTi-mix-cal catalyst, indicating its excellent selectivity.

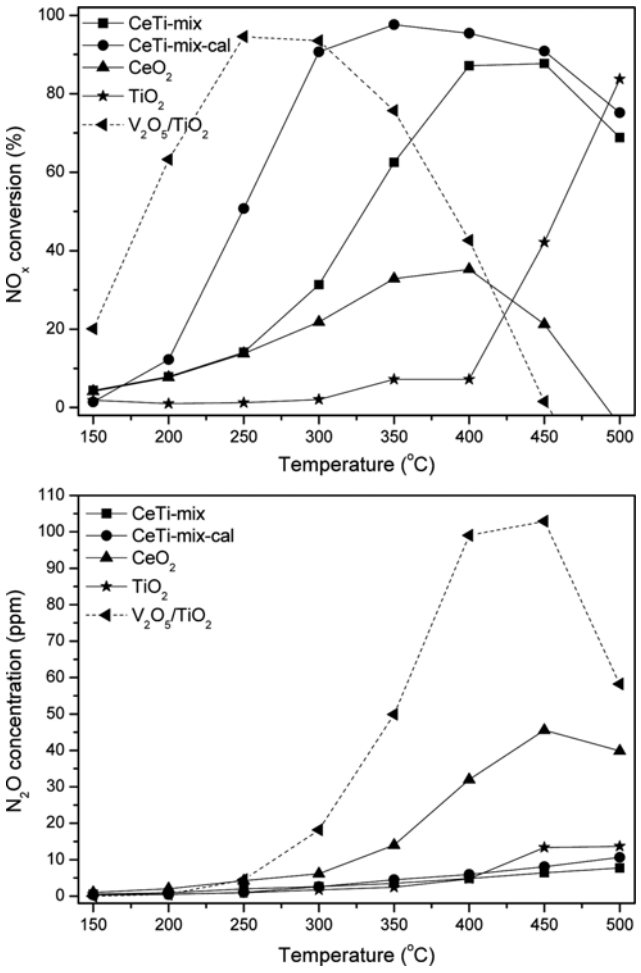

Fig. 1. NO_x conversion and N_2O concentration of various samples in NH_3-SCR as a function of temperature.

In a real exhaust gas condition, the presence of H_2O often leads to the deactivation of the SCR catalyst. Especially, the operating

window of metal oxide catalysts, such as vanadia or ceria based materials, are prone to be shifted toward high temperature, which might be attributed to the competitive adsorption of H_2O and NH_3 molecules on the acid sites at relatively low temperature [12,13]. Thus, the effect of H_2O on the SCR activity of CeTi-mix-cal sample was investigated at 300 °C and 350 °C as shown in Fig. 2. When 3% H_2O was fed into the inlet gas at 300 °C, NO_x conversion decreased to about 60% and remained at that level for 12 h. After H_2O was excluded from the stream, however, the value of NO_x conversion rapidly recovered to the initial level. In the case of reaction at 350 °C, water vapor slightly inhibited the SCR activity but NO_x conversion was still maintained above 90% for 12 h. Similarly, the NO_x conversion was recovered after removing H_2O from the feed gas. Thus, it was shown that CeTi-mix-cal sample had stable SCR performance in the presence of H_2O for a long time, which is favorable for practical application.

2. Characterization

2-1. XRD Results

Fig. 3 shows XRD patterns of CeO_2, TiO_2, CeTi-mix, and CeTi-mix-cal samples. In the case of TiO_2, dominant peaks at 2θ=25.3° and 37.8° are clearly observed, which corresponds to anatase TiO_2

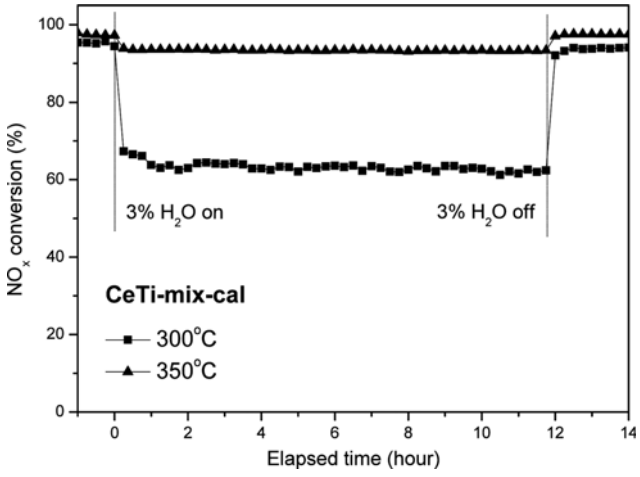

Fig. 2. NH_3-SCR activity over CeTi-mix-cal sample in the presence of H_2O at 300 °C and 350 °C under GHSV of 80,000 mL g^{-1} h^{-1}.

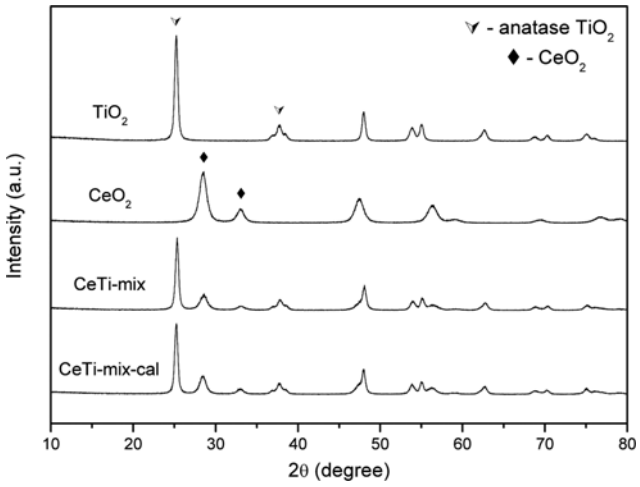

Fig. 3. Powder-XRD patterns of various samples.

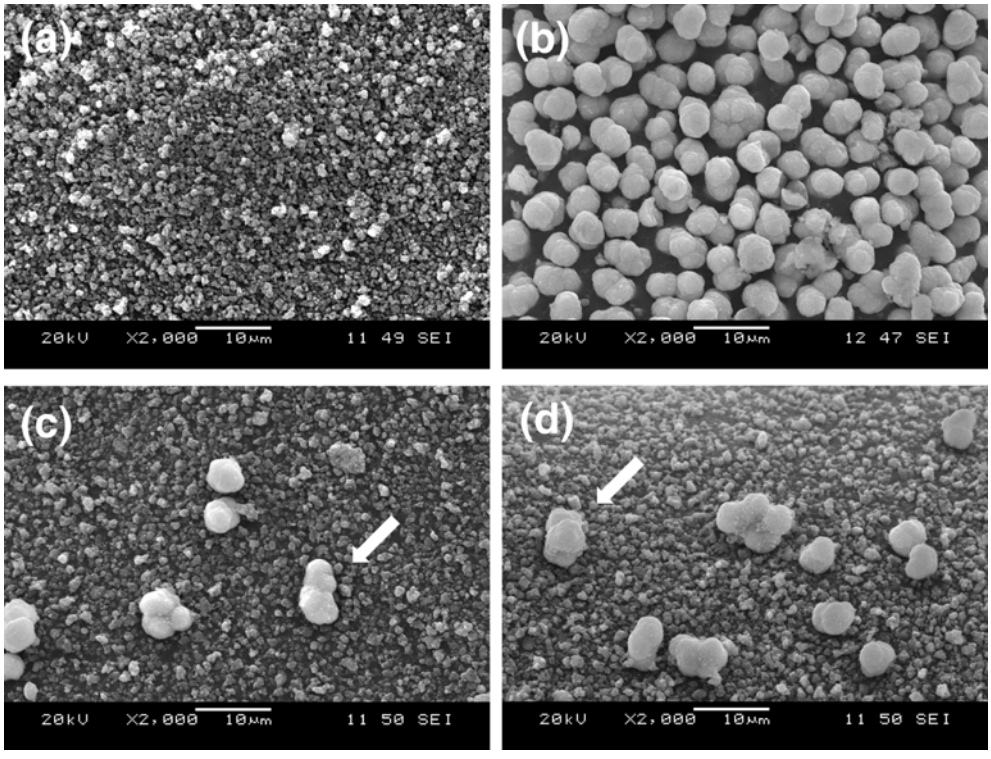

Fig. 4. SEM images of (a) TiO_2, (b) CeO_2, (c) CeTi-mix and (d) CeTi-mix-cal. Arrow indicates circular CeO_2 particles in the mechanical mixtures (c) and (d).

phase (PDF #21-1272). CeO_2 has the cubic phase with a fluorite structure, as evidenced from the peaks at 2θ=28.6° and 33.1° (PDF #65-5923). After these two samples were mechanically mixed, each of them maintained its own phase with similar broadness, which indicated that the size of crystalline domain was not affected by the simple mechanical mixing procedures. In addition, the subsequent calcination of the mechanical mixture at 500 °C had no effect on the phase or crystalline size of each particle. It means that the calcination of the mechanical mixture at 500 °C did not induce the particular interaction between CeO_2 and TiO_2 in the level of the crystalline domain.

2-2. SEM-EDS Results

The morphology of CeO_2, TiO_2, and their mechanical mixture was analyzed with SEM investigation. Interestingly, CeO_2 and TiO_2 samples used in this study have noticeable difference in size and morphology, which makes two particles clearly distinguishable in SEM image. Fig. 4(a) shows that TiO_2 particles have random shape and size within 1-2 μm. In contrast, CeO_2 particles have relatively narrow size distribution between 4-5 μm with circular morphology. After mechanical mixing (Fig. 4(c) and 4(d)), it is confirmed that two particles maintained their own morphology without sintering. This result is well consistent with the XRD analysis. It is widely accepted that the interaction between Ce and Ti in atomic scale (e.g. Ce-O-Ti bond) is the important factor to determine the activity for Ce-Ti based catalyst [14]. The mechanical mixture of CeO_2 and TiO_2 in this study, however, is not expected to produce molecular level mixing between Ce and Ti like one prepared by sol-gel method, for example. Hence, the enhanced catalytic activity of CeTi-mix-cal in this study must be explained by other factors.

The compositions of each particle before and after mechanical mixing were investigated with EDS analysis. Data obtained from 20 different points were averaged to compare the concentration of each element in the samples with the mean absolute deviation as summarized in Table 1. About 2.0 atomic % of S was detected in commercial TiO_2, although no sulfur was detected over CeO_2. Interestingly, when the X-ray was intentionally focused on several spots in CeO_2 particles of CeTi-mix sample, the average amount of sulfur content was 2.2 atomic %, which was higher value than expected. If we assume that sulfate ions are immobilized on TiO_2 surface, nearly 0.3% of S should be detected on CeTi-mix sample considering that initial atomic ratio of Ti to S in TiO_2 itself was 98 to 2 and 14.1% of Ti was detected in CeTi-mix sample. However, 2.2% of S was detected in a region centered at CeO_2 particles, indicating that there was a certain change in sulfur distribution in the mixture of TiO_2 and CeO_2 particles. It means that sulfate species were bound not only to TiO_2 but also to CeO_2 in CeTi-mix sample. Furthermore, in the case of CeTi-mix-cal sample, S to Ce ratio increased by almost two-times higher than that in CeTi-mix sample, so mechanical mixing and the subsequent calcination at 500 °C facilitated the migration of sulfate species from TiO_2 to CeO_2 particles, resulting in more populated sulfate species on CeO_2. Thus, it could be suggested that the enhanced SCR activity of CeTi-mix-cal and CeTi-mix particles might be attributed to the formation of sulfate species on CeO_2 particles.

2-3. H_2-TPR Results

Fig. 5 shows H_2-TPR profiles of the prepared samples. TPR profile of TiO_2 sample shows a reduction signal between 490 °C and 610 °C, which can be assigned to the reduction of sulfate species on TiO_2 particles [15]. This reduction peak comprises several sub-signals, indicating the heterogeneity in the surface sulfate species on TiO_2. TPR profile of CeO_2 sample represents two reduction peaks at 466 °C and 819 °C, which can be assigned to the reduction of surface oxygen species and bulk oxygen in the lattice of CeO_2, respectively [16]. Meanwhile, CeTi-mix and CeTi-mix-cal samples show significantly different reduction behavior compared to TiO_2

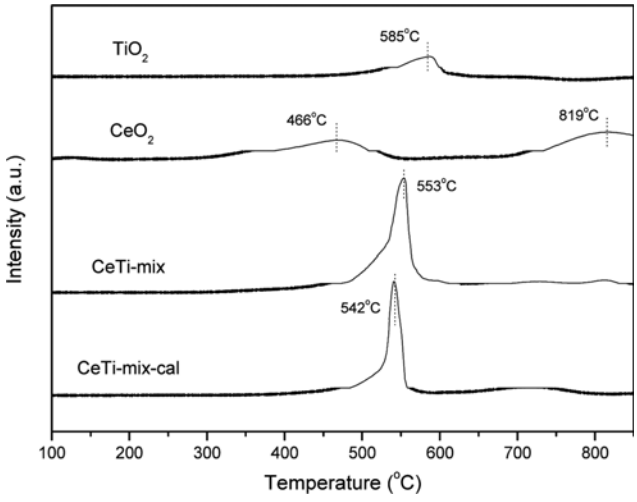

Fig. 5. H_2-TPR profiles over TiO_2, CeO_2, CeTi-mix and CeTi-mix-cal samples.

Table 1. Atomic percentages of Ce, Ti and S on TiO_2, CeO_2, CeTi-mix and CeTi-mix-cal particles determined from EDS analysis by averaging the compositions of twenty points

Sample	Ce		Ti		S		S/Ce (molar ratio)
	Average	Δ^b	Average	Δ^b	Average	Δ^b	
TiO_2	0	-	98.0	0.7	2.0	0.7	-
CeO_2	100.0	0	0	-	0	-	-
CeTi-mix[a]	83.7	3.7	14.1	3.7	2.2	0.8	0.03
CeTi-mix-cal[a]	79.5	3.1	15.7	3.4	4.8	0.4	0.06

[a]X-ray was intentionally focused on CeO_2 particles in these mixtures

[b]Mean absolute deviation was calculated from following Eq. ($\Delta = \frac{1}{20}\Sigma_{i=1}^{20}|x_i - \bar{x}|$)

or CeO_2. These two samples do not have a peak arising from reduction of surface oxygen species in CeO_2. On the other hand, a strong signal at 542 °C appears originating from the reduction of sulfated CeO_2 as previously reported [7]. Also, there is a slight difference in the reduction peak position between CeTi-mix and CeTi-mix-cal samples. The reduction peak of CeTi-mix-cal is located at 542 °C, while that of CeTi-mix is at 553 °C, implying that the sulfate species on the former sample has a more similar characteristic to cerium sulfate than one on the latter. Therefore, TPR analysis demonstrates that sulfur species on TiO_2 are migrated to CeO_2 by mechanical mixing and the subsequent calcination, resulting in the formation of more stable sulfated CeO_2 which is consistent with the EDS results.

2-4. NH_3-TPD Results

A standard SCR reaction over metal oxide catalysts usually occurs with Eley-Rideal mechanism, which means that gaseous NO molecules are reduced by interacting with adsorbed NH_3 molecules on the acid sites [13]. Therefore, the quantity and strength of acid sites are important factor in determining the reaction behavior over metal oxide catalysts. Earlier we confirmed that just mechanical mixing and subsequent calcination of the mixture of CeO_2 and TiO_2 led to enhanced activity in SCR reaction. To investigate the change of acid site distribution of catalysts before and after mixing and after-treatment, NH_3-TPD experiments were carried out as shown in Fig. 6. For this experiment, CeO_2 and TiO_2 were mechanically mixed with the mass ratio of 1 : 1 to clarify the effect of sulfate migration. Experimental details are described in the experimental section.

In the case of TiO_2, with a small amount of sulfate, a large desorption peak of NH_3 occurred in a wide range from 100 to 500 °C. In contrast, slight desorption of NH_3 appeared between 100 and 300 °C in pure CeO_2. The sum of two desorption spectra was suggested as CeO_2+TiO_2 in Fig. 6. Interestingly, after this mixture was calcined, the amount of NH_3 desorbed from 100 to 300 °C considerably increased compared to the sum of desorption peak from pure CeO_2 and TiO_2, whereas NH_3 desorbed above 400 °C almost disappeared in CeTi-mix-cal sample. This result implies that the migration of sulfate species from TiO_2 to CeO_2 can lead to the redistribution of acid sites and their strength because the acidic properties generated by sulfate species are strongly affected by the environment of sulfate, such as support and surface coverage. The reduction of strong acid sites above 400 °C may arise from the loss of sulfate on TiO_2, and the newly formed sulfated CeO_2 is the main reason for the increased amount of acid sites at low temperature around 200 °C. In addition, the previous results on NH_3-TPD of sulfated CeO_2 and sulfated TiO_2 reported that NH_3 adsorbed on the latter is more thermally stable than that on the former [7,17], which is well consistent with our result. It can be claimed that such change in the distribution of acid sites and acid strength of CeTi-mix-cal sample is related to its enhanced deNO_x activity.

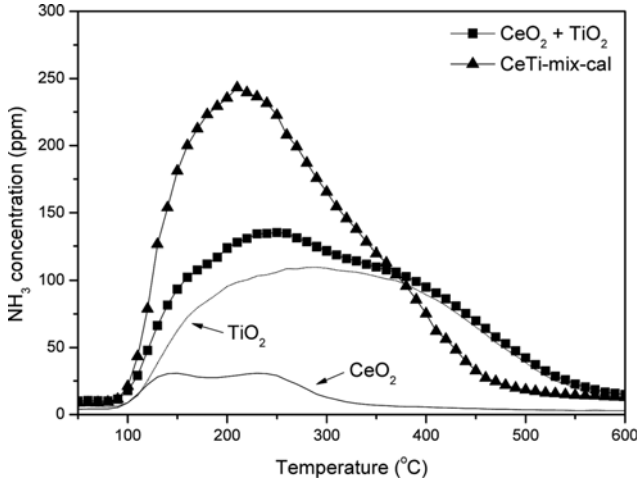

Fig. 6. NH_3-TPD profiles over TiO_2, CeO_2 and CeTi-mix-cal samples. For this experiment, 0.07 g of sieved samples was used for pure CeO_2 or TiO_2 sample, and 0.14 g of sample was used for CeTi-mix-cal.

3. Observation of the Migration of Sulfate Species

3-1. SO_2 Desorption Profile

It has been known that the stability of sulfate species on CeO_2 and TiO_2 surface is different [11,18], which leads us to compare the SO_2 desorption behavior resulting from the decomposition of sulfate during the temperature ramping. For this experiment, CeO_2 and TiO_2 were mechanically mixed with the mass ratio of 1 : 1 to disambiguate and clarify the difference between sulfate on TiO_2 and sulfated CeO_2, which is similar to the NH_3-TPD experiment. Thus, the amount of SO_2 desorbed from TiO_2 should be two-times higher than that from CeTi-mix. SO_2 desorption profiles of TiO_2 and CeTi-mix samples with increasing temperature up to 850 °C are displayed as shown in Fig. 7. In case of TiO_2, SO_2 began to be desorbed around 620 °C with the maximum at 760 °C. If the sulfate species are immobilized at the initial position, e.g., TiO_2, these two samples must have demonstrated the same desorption characteristics. However, CeTi-mix did not emit SO_2 until the temperature reached 800 °C, above which the amount of SO_2 desorption rapidly increased, probably attributed to the decomposition of newly formed sulfated CeO_2. Meanwhile, Waqif et al. reported that bulk type sulfate species on CeO_2 were decomposed to produce SO_2 at 600 °C under vacuum condition, while surface type sulfate species persisted even after evacuation at 700 °C for 15 min [11]. Therefore, it can be summarized that most of sulfate species in the CeTi-mix sample exist as surface sulfate on CeO_2 as evidenced by the SO_2 desorption results.

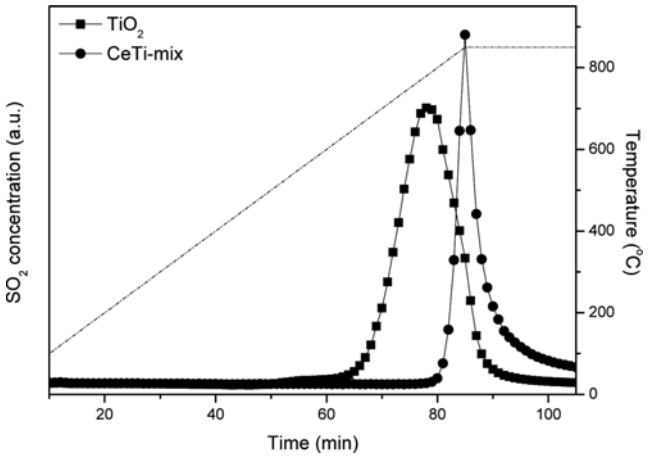

Fig. 7. SO_2 desorption profiles of TiO_2 and CeTi-mix samples.

Based on these results, it is obvious that either sulfur species on TiO_2 or sulfur species on CeO_2 cannot be decomposed into SO_2 in oxidative condition at 500 °C up to which the SCR reaction takes place. For the case of CeTi-mix-cal sample, moreover, sulfate species exist on CeO_2, which means that sulfate species are mobile on the surface and diffuse to other particles via inter-particle migration during the simple mechanical mixing treatment. Considering that the desorption temperature of SO_2 on CeO_2 is higher than that of SO_2 on TiO_2 by 200 °C, sulfate species on CeO_2 is expected to be more stable than those on TiO_2, which can act as the driving force of sulfate migration. Also, such inter-particle migration of sulfate species was further facilitated by the subsequent calcination treatment.

3-2. *In situ* DRIFT Study

It is difficult to evidently identify the migration of sulfate species in the samples by examining the change in IR band of sulfate species because there are many other IR bands overlapped with that of sulfate if IR spectrum is taken at ambient condition. Hence, the temperature-resolved DRIFT (Diffuse reflectance infrared Fourier transform) experiment over TiO_2 and CeO_2 particles were applied to remove the impurity in the sample. Note that the sulfate species are stable up to 500 °C as confirmed in the SO_2 desorption experiment (Fig. 7). The spectrum of each sample taken at room temperature was used as a background spectrum (Fig. 8). Samples were heated to 500 °C with a ramping rate of 10 °C/min in 5% O_2 balanced with N_2.

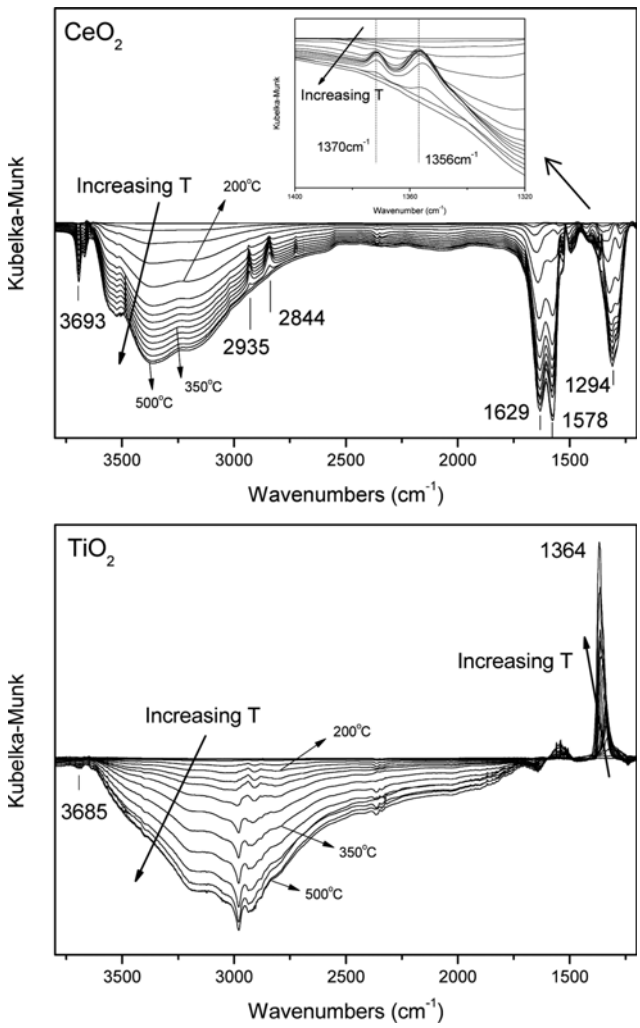

Fig. 8. Temperature-resolved DRIFT spectra over (up) CeO_2 and (down) TiO_2 particles. Samples were heated to 500 °C at the ramping rate of 10 °C/min, and spectra were obtained at an interval of 30 °C.

With increasing temperature up to 500 °C, CO, NO and H_2O gas were desorbed from the CeO_2 surface (not shown), originating from the decomposition of the adsorbed carbonate and nitrate species on uncalcined CeO_2 surface. As demonstrated in Fig. 8, the band at 1,629 cm^{-1}, assigned to nitrite, and the bands at 1,578 and 1,294 cm^{-1}, assigned to bidentate and monodentate nitrate, respectively [19,20] disappeared at elevated temperature. Also, the broad bands from 3,000 to 3,600 cm^{-1} were gradually gone, indicating the disappearance of hydrogen bonding between water molecules and ceria surface [21]. A sharp peak at 3,693 cm^{-1} corresponding to the free OH bond of water molecules also decreased at elevated temperature, implying the desorption of H_2O, or dehydration, at elevated temperature. In particular, the bands at 1,550 and 1,370 cm^{-1}, which could be assigned to bidentate formate, and the bands at 1,530 and 1,356 cm^{-1}, which could be to bidentate carbonate, gradually appeared from 160 °C [22,23]; however, these peaks finally disappeared at 470 °C. Removal of such peaks is important, because the IR band of S=O bond in sulfate is superimposed in the region. Except for such carbon-related species, no new peaks appeared over the whole temperature region.

In the case of TiO_2, H_2O and a small amount of NH_3 gas were desorbed from the surface with increasing temperature (not shown). Similar to CeO_2, the sharp peak at 3,685 cm^{-1} corresponded to the free OH bond of water molecules, and the broad band at 2,700 to 3,300 cm^{-1} could be assigned to the hydrogen bonding between ammonia or water and TiO_2 surface, as displayed in Fig. 8. Interestingly, a very sharp band at 1,364 cm^{-1} appeared with increasing temperature, which could be attributed to the stretching frequencies of S=O bond in sulfate species [24,25]. The formation of S=O species with increasing temperature is rationalized by the following reaction between bisulfate and hydroxyl group on TiO_2.

$$[O=SO_2-OH]^- + OH^- \leftrightarrow [O=SO_2=O]^{2-} + H_2O$$

As shown in Fig. 8, uncalcined catalyst contains the large amount of water on its surface at low temperature. Protons originating from adsorbed water molecules on the TiO_2 surface can exist as bisulfate groups (HSO_4^-) or as hydroxyl groups (OH^-) bridging Ti metal ions. When the temperature increases, hydroxyl group on the catalyst surface can interact with the adjacent bisulfate ion to form sulfate ion on the surface and water molecule in gas phase [26].

Keeping this phenomenon in mind, *in situ* DRIFT spectra obtained during heating over TiO_2, CeTi-mix and CeTi-mix-cal samples were compared to analyze the band of S=O (Fig. 9, Fig. 10 and Fig. 11). For the case of TiO_2 (Fig. 9), sample was calcined at 500 °C in ambient air for 4 h to remove the impurities on the surface before measurement. As mentioned above, the band of S=O at 1,364 cm^{-1} gradually appeared with increasing temperature. The slight increase in wavenumbers of sulfate S=O bond with increasing temperature

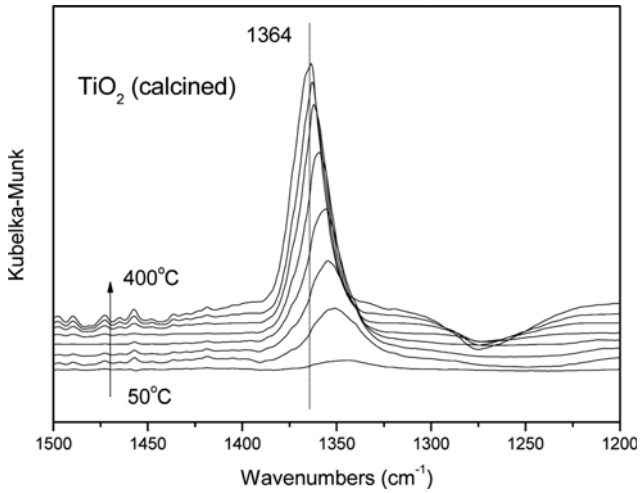

Fig. 9. *In situ* DRIFT spectra over TiO_2 calcined at 500 °C as a function of temperature. Sample was heated to 400 °C at the ramping rate of 10 °C/min, and spectra were obtained at an interval of 50 °C.

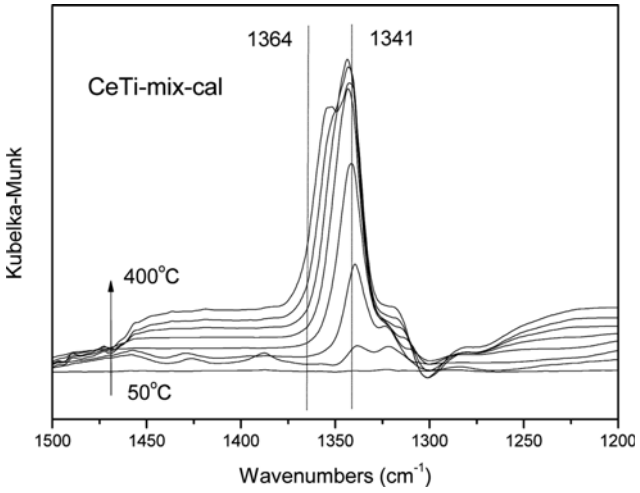

Fig. 11. *In situ* DRIFT spectra over CeTi-mix-cal as a function of temperature. Sample was heated to 400 °C at the ramping rate of 10 °C/min, and spectra were obtained at an interval of 50 °C.

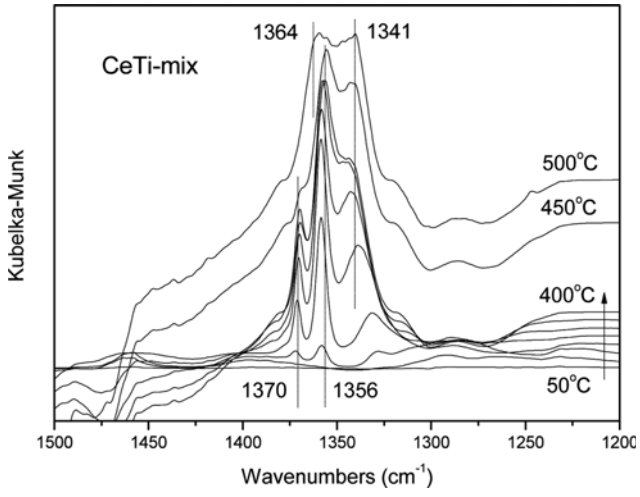

Fig. 10. *In situ* DRIFT spectra over CeTi-mix as a function of temperature. Sample was heated to 500 °C at the ramping rate of 10 °C/min, and spectra were obtained at an interval of 50 °C.

was attributed to the strengthening of S=O bond with desorption of water [27].

In the case of CeTi-mix, we aimed at observing the instantaneous change of ν(S=O) band arising from sulfate migration from TiO_2 to CeO_2. However, there were so many overlapping absorption bands which prevented the identification of S=O band; as shown in Fig. 10. Especially, two bands of formate at 1,370 cm^{-1} and carbonate at 1,356 cm^{-1}, which rapidly appeared with increasing temperature, were superimposed on the band of S=O at 1,364 cm^{-1}. Meanwhile, it is noticeable that the band at 1,341 cm^{-1} newly appeared in CeTi-mix sample with increasing temperature. Because this new peak was not shown in pure CeO_2 or pure TiO_2, it can be assigned to new sulfate on CeO_2 derived from the mechanical mixing process, also in a good agreement with the previous assignment [11]. To decompose residual carbon species, sample was heated further to 500 °C and held for a few minutes, resulting in the disappearance of the band at 1,370 cm^{-1} and 1,356 cm^{-1}. After the complete removal of carbon-related species from the surface, we found that the two bands at 1,364 and 1,341 cm^{-1} coexist, which led us to propose that the two kinds of sulfate species on TiO_2 and CeO_2 exist together for a while after calcination at 500 °C.

Finally, DRIFT spectra over CeTi-mix-cal sample were taken as a function of temperature up to 400 °C as shown in Fig. 11. Different from the above two samples (TiO_2 and CeTi-mix), CeTi-mix-cal sample demonstrated a sharp band at 1,341 cm^{-1}, which was assigned to sulfate on CeO_2, with increasing temperature, in addition to no carbon-related bands. This observation suggests that most of sulfate species exist on CeO_2 surface after mechanical mixing followed by the calcination of the mixture, which is consistent with the other characterization results described before.

In summary, the combined characterization results provide convincing spectroscopic evidence about the inter-particle migration of sulfate species from TiO_2 to CeO_2 induced by the mechanical mixing and the subsequent calcination at 500 °C. Thus, formed sulfate on CeO_2 plays an essential role in having the excellent activity as well as selectivity for SCR of NO_x with NH_3 especially in the high temperature region. Unlike previously reported methods of sulfating CeO_2 such as wet impregnation with $(NH_4)_2SO_4$ solution or exposure to SO_2 gas for a long time, our approach provides an easier and more convenient way to prepare surface type sulfate species on CeO_2 as the catalyst.

CONCLUSION

Mechanical mixtures of TiO_2 and CeO_2 samples were used as catalysts for selective catalytic reduction of NO_x with NH_3. Unlike pure CeO_2 or TiO_2, the activity of mechanical mixture was significantly improved. Especially, after calcination of the mechanical mixture at 500 °C, NO removal activity was further enhanced with

nearly 100% N_2 selectivity in the whole temperature region, which was superior to conventional V_2O_5/TiO_2 catalyst in the high temperature region. It was found that these improvements were attributed to the formation of sulfated CeO_2, as evidenced by SEM-EDS, H_2-TPR and NH_3-TPD results. The existence of sulfate species on CeO_2 was also confirmed by in situ DRIFT experiments, which could observe the change of ν(S=O) band in sulfate species from TiO_2 to CeO_2 with calcination. Furthermore, it is noticeable that the inter-particle migration of sulfate species was utilized to enhance SCR catalytic activity. This study provides the simplest way to produce sulfated CeO_2 among the previously reported methods, which can be done by simple mechanical mixing and the subsequent calcination.

ACKNOWLEDGEMENT

This project was supported by the R&D Center for reduction of Non-CO_2 Greenhouse gases (0458-20150026) funded by Korea Ministry of Environment (MOE) as Global Top Environment R&D Program. Characterization of the samples was supported by Research Institute of Advanced Materials (RIAM).

REFERENCES

1. W. N. Wan Abdullah, W. A. Wan Abu Bakar and R. Ali, *Korean J. Chem. Eng.*, **32**, 1999 (2015).
2. S. G. Lee, H. J. Lee, I. Song, S. Youn, D. H. Kim and S. J. Cho, *Sci. Rep.*, **5**, 12702 (2015).
3. S. Youn, S. Jeong and D. H. Kim, *Catal. Today*, **232**, 185 (2014).
4. S. T. Choo, I. S. Nam, S. W. Ham and J. B. Lee, *Korean J. Chem. Eng.*, **20**, 273 (2003).
5. Q. Guo, W. Jing, S. Cheng, Z. Huang, D. Sun, Y. Hou and X. Han, *Korean J. Chem. Eng.*, **32**, 2257 (2015).
6. T. Gu, Y. Liu, X. Weng, H. Wang and Z. Wu, *Catal. Commun.*, **12**, 310 (2010).
7. S. Yang, Y. Guo, H. Chang, L. Ma, Y. Peng, Z. Qu, N. Yan, C. Wang and J. Li, *Appl. Catal., B*, **136-137**, 19 (2013).
8. L. Zhang, W. Zou, K. Ma, Y. Cao, Y. Xiong, S. Wu, C. Tang, F. Gao and L. Dong, *J. Phys. Chem. C*, **119**, 1155 (2015).
9. C. Liu, L. Chen, J. Li, L. Ma, H. Arandiyan, Y. Du, J. Xu and J. Hao, *Environ. Sci. Technol.*, **46**, 6182 (2012).
10. Z. Wu, R. Jin, H. Wang and Y. Liu, *Catal. Commun.*, **10**, 935 (2009).
11. M. Waqif, P. Bazin, O. Saur, J. C. Lavalley, G. Blanchard and O. Touret, *Appl. Catal., B*, **11**, 193 (1997).
12. T. Zhang, R. Qu, W. Su and J. Li, *Appl. Catal., B*, **176-177**, 338 (2015).
13. G. Busca, L. Lietti, G. Ramis and F. Berti, *Appl. Catal., B*, **18**, 1 (1998).
14. P. Li, Y. Xin, Q. Li, Z. Wang, Z. Zhang and L. Zheng, *Environ. Sci. Technol.*, **46**, 9600 (2012).
15. P. G. W. A. Kompio, A. Brückner, F. Hipler, G. Auer, E. Löffler and W. Grünert, *J. Catal.*, **286**, 237 (2012).
16. M. Sun, G. Zou, S. Xu and X. Wang, Mater. *Chem. Phys.*, **134**, 912 (2012).
17. S. M. Jung and P. Grange, *Catal. Today*, **59**, 305 (2000).
18. O. Saur, M. Bensitel, A. B. Mohammed Saad, J. C. Lavalley, C. P. Tripp and B. A. Morrow, *J. Catal.*, **99**, 104 (1986).
19. H. Hu, S. Cai, H. Li, L. Huang, L. Shi and D. Zhang, *J. Phys. Chem. C*, **119**, 22924 (2015).
20. B. Jiang, Z. Li and S.-C. Lee, *Chem. Eng. J.*, **225**, 52 (2013).
21. L. F. Scatena, M. G. Brown and G. L. Richmond, *Science*, **292**, 908 (2001).
22. S. Bailey, G. F. Froment, J. W. Snoeck and K. C. Waugh, *Catal. Lett.*, **30**, 99 (1995).
23. J. Xu, Y.-Q. Deng, X.-M. Zhang, Y. Luo, W. Mao, X.-J. Yang, L. Ouyang, P. Tian and Y.-F. Han, *ACS Catal.*, **4**, 4106 (2014).
24. P. Bazin, O. Saur, F. C. Meunier, M. Daturi, J. C. Lavalley, A. M. Le Govic, V. Harlé and G. Blanchard, *Appl. Catal., B*, **90**, 368 (2009).
25. L. Zhang, L. Li, Y. Cao, X. Yao, C. Ge, F. Gao, Y. Deng, C. Tang and L. Dong, *Appl. Catal., B*, **165**, 589 (2015).
26. B. Li and R. D. Gonzalez, *Catal. Today*, **46**, 55 (1998).
27. C. E. Nanayakkara, J. Pettibone and V. H. Grassian, *Phys. Chem. Chem. Phys.*, **14**, 6957 (2012).